EFDA–JET–CP(12)06/24

M.N.A. Beurskens, L. Frassinetti, C. Maggi, G Calabro, B. Alper, C. Angioni, C. Bourdelle, S. Brezinsek, P. Buratti, C. Challis, T. Eich, J. Flanagan, E. Giovannozzi, C. Giroud, M. Groth, J. Hobirk, E Joffrin, M.J. Leyland, P. Lomas, E. de la Luna, M. Kempenaars, P. Mantica, M. Maslov, G. Matthews, M-L Mayoral, R. Neu, I. Nunes, T. Osborne, F. Rimini, S. Saarelma, R. Scannell, E.R. Solano, P.B. Snyder, I. Voitsekhovitch, Peter de Vries and JET EFDA contributors

L-H Power Threshold, Confinement, and Pedestal Stability in JET with a Metallic Wall

L-H Power Threshold, Confinement, and Pedestal Stability in JET with a Metallic Wall

M.N.A. Beurskens[1], L. Frassinetti[2], C. Maggi[3], G Calabro[4], B. Alper[1], C. Angioni[3], C. Bourdelle[5], S. Brezinsek[6], P. Buratti[4], C. Challis[1], T. Eich[3], J. Flanagan[1], E. Giovannozzi[4], C. Giroud[1], M. Groth[7], J. Hobirk[3], E Joffrin[5], M.J. Leyland[8], P. Lomas[1], E. de la Luna[9], M. Kempenaars[1], P. Mantica[10], M. Maslov[1], G. Matthews[1], M-L Mayoral[1], R. Neu[3], I. Nunes[11], T. Osborne[12], F. Rimini[1], S. Saarelma[1], R. Scannell[1], E.R. Solano[10], P.B. Snyder[12], I. Voitsekhovitch[1], Peter de Vries[13] and JET EFDA contributors*

JET-EFDA, Culham Science Centre, OX14 3DB, Abingdon, UK

[1]EURATOM-CCFE Fusion Association, Culham Science Centre, OX14 3DB, Abingdon, OXON, UK
[2]Division of Fusion Plasma Physics, Association EURATOM-VR , KTH, SE-10044 Stockholm, Sweden
[3]Max-Planck-Institut für Plasmaphysik, EURATOM Association, D-85748 Garching, Germany
[4]Associazione EURATOM -ENEA sulla Fusione, C.R. Frascati, Frascati, Italy
[5]Association EURATOM-CEA, IRFM, F-13108 St-Paul-Lez-Durance, France
[6]Association EURATOM/Forschungszentrum Juelich GmbH 52425 Juelich Germany
[7]Association EURATOM/Helsinki University of Technology 02015 Espoo Finland
[8]Department of Physics, University of York, Heslington, York, YO10 5DD, UK
[9]Laboratorio Nacional de Fusion, Asociacion EURATOM-CIEMAT, Madrid, Spain
[10]Istituto di Fisica del Plasma 'P.Caldirola', Associazione Euratom-ENEA-CNR, Milano, Italy
[11]Centro de Fusao Nuclear, Associacao EURATOM-IST, Lisboa, Portugal
[12]General Atomics, PO Box 85608, San Diego, California 92186-5608, USA
[13]Association EURATOM/DIFFER, Rijnhuizen P.O. Box 1207 3430BE Nieuwegein, Netherlands
** See annex of F. Romanelli et al, "Overview of JET Results", (24th IAEA Fusion Energy Conference, San Diego, USA (2012)).*

Preprint of Paper to be submitted for publication in Proceedings of the
24th IAEA Fusion Energy Conference (FEC2012), San Diego, USA
8th October 2012 - 13th October 2012

ABSTRACT

The power P_{thr} required for the L-H transition has reduced by over 30% in JET with the ITER like Be/W wall (JET-ILW) compared to Pthr in JET with the Carbon wall (JET-C). In addition, density scans in JET-ILW show that P_{thr} increases below a minimum pedestal density, which was not found in JET-C. The confinement factor $H_{98,y2}$ in Type I ELMy H-mode baseline plasmas is lower in JET-ILW compared to JET-C at low power fractions $P_{net/Pthr,08} < 2$ (where Pnet is the net input power, and $P_{thr,08}$ the L-H power threshold from [21]). However, at $P_{net}/P_{thr,08} > 2$, the confinement in JET-ILW (mainly hybrid plasmas) is similar to that in JET-C. In general the pedestal pressure in JET-ILW is reduced compared to JET-C baseline and hybrid H-modes. This is the main reason for the reduced confinement in JET-ILW baseline ELMy H-mode plasmas where typically $H_{98,y2} = 0.8$ is obtained, compared to $H_{98,y2} = 1.0$ in JET-C. In JET-ILW hybrid plasmas the reduced pedestal pressure is compensated by an increased peaking of the core pressure profile resulting in $H_{98,y2} \leq 1.25$. The pedestal stability in JET baseline ELMy H-mode plasmas is consistent with the calculated Peeling Ballooning stability limit, although uncertainties in the ion dilution and edge impurity content render this analysis inconclusive. Nevertheless a database comparison of predictions using the EPED model with measured pedestal pressures in over 500 JET-C and JET-ILW baseline and hybrid plasmas shows a good agreement with $0.8 <$ (measured p_{ped}) / (predicited $p_{ped,EPED}$) < 1.2.

1. INTRODUCTION.

In preparation for ITER, JET's main plasma facing components, previously of carbon (JETC), have been replaced with a new ITER-like wall (JET-ILW), with mostly Be in the main chamber and W in the divertor [22]. This paper reports on recent JET studies on the influence of the ILW on the L-H power threshold P_{thr} (the total required net input power to get an L-H transition) at low plasma density (n_e)

The input power, $P_{H=1}$, required above the L-H threshold to get good confinement H~1 is also important for ITER as it indicates the required installed input power. In JET-C the power required to get H_{98}~1 (using IPB98(y,2), [14]) varied as $1.3\text{-}2 \times P_{thr}$ [26] depending on the plasma triangularity. The hope is that if P_{thr} is reduced JET-ILW also $P_{H=1}$ would be reduced.

This paper will discuss dedicated experiments on the L-H power threshold in JET-ILW and discusses the confinement properties of the established H-modes in terms of global, pedestal and core confinement. It also investigates the pedestal stability in H-modes in JETILW and compares the achieved pedestal confinement with that predicted by modelling.

2. L-H TRANSITION AND ACCESS TO TYPE I ELMY H-MODE WITH C AND BE/W WALL.

An L-H transition experiment was conducted in JET-C and JET-ILW in plasmas with low triangularity δ_{av}~0.25 [19]. The plasma density was varied from shot to shot to obtain an overlap in density range. Slow input power ramps (ICRH or NBI), typically 1MW/s, were used to measure $P_{thr} = P_{in}$-dW/dt.

In JET-C at 1.8T/1.7MA, P_{thr} is found to be consistent with the multi machine scaling $P_{thr,08}$ [21]. Conversely, in density scans in JET-ILW Pthr increases below a minimum pedestal density, $n_{e,min} \sim 2.2\times10^{19}$ m^{-3}, as shown in Figure 1. In order the correct for plasma radiation losses we also compare the power crossing the separatrix $P_{sep} = P_{thr} - P_{rad,bulk}$ (the main plasma radiated power) ; the minimum in required P_{sep} still occurs at ne,min. In addition, the difference in P_{thr} between the ICRH and NBI heated plasmas disappears in doing so as $P_{rad,bulk}$ is larger with ICRH than with NBI due to an increase in the W and Ni radiation at low density.

The increase of Pthr below ne,min was first observed with the MkII-GB divertor [11, 1]. However, after removal of the divertor septum (MkIIGB SRP) [1] and, more recently, with the current MkII-HD divertor geometry no roll-over of P_{thr} was found at low density [15]. With the ILW the minimum has thus been recovered, but the physics behind this process in not well understood.

At plasma densities above ne,min, Pthr is reduced by ~30% compared to $P_{thr.08}$ and P_{sep} by ~40% in JET-ILW compared to JET-C. A similar, strong influence of the wall change from C to Be/W on P_{thr} and P_{sep} is also observed at 3.0T/2.75MA. In addition, ne,min ~ 3.5×10^{19} m^{-3} at 3.0T, having increased roughly linearly with B_T (at constant q_{95}). This is relevant to ITER, which needs to access the H-mode at high magnetic field ($B_T = 5.3$T); indicating that a minimum density is required to obtain an H-mode with minimum input power.

In addition to a sufficiently low L-H power threshold in ITER, access to plasmas with a confinement enhancement factor of $H_{98}\approx1$ is required for ITER to achieve Q = 10 in its baseline H-mode scenario at 15MA. A separate experiment was conducted to get a controlled transition from Type I to Type III ELMs through a fuelling ramp at constant input power [12]. Two plasmas are compared at B_T = 3T an I_p = 2MA for JETC (P_{net} = 10MW) and JET-ILW (P_{net} = 8MW). As the fuelling is increased the plasma density increases and the H-mode confinement is degraded. Hyperbolic tangent fits to High Resolution Thomson Scattering (HRTS) pedestal profiles are used to monitor the pedestal density and temperature evolution. As the pedestal density is increased due to the fuelling the pedestal temperature is reduced at a faster rate such that the pedestal pressure decreases, Figure 2. For JET-C a transition from Type I to Type III ELMs occurs at a pedestal temperature of Te,ped ≈ 650eV. In JET-ILW a transition from Type I ELMs to a type III ELMs is observed at a much lower temperature $T_{e,ped} \approx 280$eV. This comparison shows that the critical temperature model for the Type I to Type III transition [13, 26, 7] does not describe these observations. In JET-ILW the confinement factor is $H_{98} \approx 0.8$ with type I ELMs and $H_{98} \approx 0.6$ during the Type III ELMs. In comparison, JET-C experiments featured $H_{98} \approx 1.0$ and $H_{98} \approx 0.8$ during the Type I and III ELM periods respectively.

3. CONFINEMENT IN CFC AND ILW TYPE I ELMY H-MODE PLASMAS

In JET-ILW both the baseline and the hybrid Type I ELMy H-mode plasma scenarios have been (re-)developed at low and high plasma triangularity [16, 17]. A confinement database for these scenarios containing 115 H-mode plasmas in the JET-C is described in [5, 3]. A JET-ILW scenario confinement database has been constructed with over 400 baseline H-mode and hybrid plasmas. An

overview of the covered triangularity, safety factor (q_{95}) and plasmas currents are given in Table 1. Only plasmas identified as Type I ELMy H-modes have been included in the database. Operation with the Be/W wall has lead to a narrower access to stable plasma operation, where higher fuelling levels are required than in the carbon wall experiments [17, 24].

The Hybrid plasmas have $q_{95} = 3.5$-4.5 and feature early heating and a current overshoot before the heating phase in order to shape the current profiles and to avoid large sawtooth activity and, at least temporarily, avoid the generation of confinement compromising m/n=3/2 and 4/3 NTM activity [10]. Thanks to the high input power and low plasmas current in these plasmas, high values of normalized pressure can be achieved up to $\beta_N \leq 3.5$. The baseline ELMy H-mode plasmas typically operate with $\beta_N \leq 2$ and have $q_{95} = 2.8$–3.6. They do not feature any current profile shaping, and have a late onset of the additional heating. Each of the scenarios are described in detail in [17]; A comparison of H_{98} as a function of the ratio of $P_{NET}/P_{thr,08}$ is shown in Figure 3. In the ILW experiments the Type I ELMy H-mode is accessible at input powers below $P_{thr,08}$, consistent with the findings in Section 2 where $P_{thr} < P_{thr,08}$ for JET-ILW. Importantly, at low $P_{NET}/P_{thr,08}$ low confinement is obtained in the ILW and $H_{98} \approx 1$ only occurs at $2<P_{net}/P_{thr,08}<3$.

The database contains a degree of overlap between hybrid plasmas at low input power and low confinement factor ($H_{98} \approx 0.8$) and baseline plasmas at high input power and good confinement ($H_{98} \approx 1.0$). Figure 4 shows the energy confinement time τe normalised to the τ_{98} scaling as $I_p^{0.93} B_t^{0.15} n_e^{0.41}$. In JET-C the hybrid and baseline plasmas are off-set as the baseline plasmas feature a lower H98 than the hybrid plasmas, but both scenarios follow a similar power degradation consistent with the τ_{98} scaling of $P^{-0.69}$. The JET-ILW baseline Hmode plasmas lie on a lower power degradation "branch" compared to the CFC-plasmas. However, at increased input power (for a reduced data set with $I_p < 2.1$MA) a smooth transition occurs towards the higher confinement "branch". This observation suggests that a certain minimum input power is required in order to recover a similar confinement as was achieved in JET-C.

4. CORE CONTRIBUTION TO CONFINEMENT

The role of the core confinement is studied by a comparing the T_e and n_e profile shapes. The so-called peakedness of the profiles is studied (defined as the ratio of the profile values at a radius $\rho_{tor} \sim 0.4$ and at $\rho_{tor} \sim 0.8$), using JET HRTS data. The ion temperature profiles from Charge Exchange recombination spectroscopy are not yet available for the ILWdatabase.

For JET-C, a strong degree of pressure profile peaking conservation was observed across the scenarios, [3]. This was caused by a flattening of the density profile, and a steepening of the temperature profiles with increasing effective collisionality ν_{eff}($\nu_{eff} = 1 \cdot 10^{14} \cdot R_{geo} \cdot z_{eff} \cdot \langle n_e \rangle / \langle T_e \rangle^2$, where $\langle n_e \rangle$ and $\langle T_e \rangle$ are volume averaged, and R_{geo} is the geometrically averaged major radius).

For JET-ILW, the trend in density peaking is well reproduced, Figure 5, (left figure). However the temperature profile peaking no longer compensates the density flattening with collisionality, and the pressure peaking is no longer conserved. Figure 5, (right figure), shows that whereas the

baseline plasmas feature a similar peaking of T_e and n_e for JET-C and JET-ILW, the confinement contribution due to core temperature profile peaking is enhanced for the hybrid plasmas in JET-ILW compared to JET-C hybrid plasmas.

5. PEDESTAL CONTRIBUTION TO CONFINEMENT

The electron pedestal densities, ne,ped and temperatures $T_{e,ped}$ from hyperbolic tangent fits to HRTS profiles are shown in Figure 6 (left) for the CFC database. The hybrid pedestal plasmas are hot and have low plasma density, whereas the baseline H-mode pedestal plasmas are cooler and denser. As I_p varies in the database a normalisation to the plasma current is performed by comparing the Greenwald density fraction $n_{e,ped}/n_{gw}$ ($\sim n_{e,ped}/I_p$) with T_{ped}/I_p to enable a comparison of the data along curves of constant pedestal poloidal pressure $\beta_{pol,ped}$ (which scales as $1/I_p^2$).

The ILW pedestal data is overlaid to the CFC data in Figure 6 (right). A first observation is that most ILW plasma scenarios have a lower maximum achieved Te,ped compared to their CFC counterpart, which is not (completely) compensated by ne,ped. Hence the pedestal confinement is reduced for the ILW plasmas. For the high performance hybrid plasmas this is compensated by increased core pressure profile peaking, whereas for the baseline plasmas the core profile peaking in the ILW plasmas is at a similar level as that of the CFC baseline plasmas.

6. PEDESTAL STABILITY AND COMPARISON WITH MODELLING

The ILW experiment has given access to Type I ELMy H-mode operation in a low confinement state with $H_{98} \approx 0.8$, previously the domain of Type III ELMy H-mode in JET with the CFC. The ELMs have been classified as Type I following the simple rule that fELM increases with increasing input power (while Type III ELMs are characterised as FELM decreasing with increasing input power), [24]. Other evidence for the ELM type classification as Type I is provided by the size of the individual ELM losses $\Delta W_{ped}/W_{ped}$, $\Delta T_e/T_e$ and $\Delta n_e/n_e$ which are significant and of the order of 10–20% in the ILW database, again typical for Type I ELMs. An important difference that has often been observed in the ILW Type I ELMy H-modes is that the ELM collapse time scale is much longer than previously observed in CFC plasmas. In [18] it was reported that the typical 'duration' of the ELM event in JET with the carbon wall is 200μs and was seen in e.g. the pedestal electron temperature collapse. Figure 7 (left) show the duration of the ELM collapse for a Type I ELMy H-mode in the ILW with I_p/B_t = 2.5MA/2.7T high triangularity ($\delta \sim 0.42$, P_{net} = 15MW) baseline plasma (Pulse No: 82806). The figure shows that the ELM collapse has a longer time scale. The initial drop has a time scale of ~2ms, i.e. ten times longer than that observed in JET with the CFC wall. A subsequent further loss occurs for some of the ELMs with a time scale of 5–10ms. This secondary collapse is not further discussed here, and is thought to be is related to an extended period of reduced confinement. Slow ELMs are potentially good news as they result in reduced peak heat loads to the divertor components.

The Peeling Ballooning stability of the pre-ELM pedestal profiles (obtained from fits to HRTS

Te and ne profiles in the last 30% of the ELM cycle [6]) has been determined with the linear MHD stability code ELITE [Snyder-NF-2004] for the same discharge. Figure 7 (right) shows the jped-α diagram for this plasma. It is found that the pedestal is 'stable' against the Peeling Ballooning boundary which is a-typical for JET Type I ELMy H-mode plasmas [25, 2, 7]. However, we note that the uncertainty in the measured profiles, particularly in the absence of ion measurements and impurity density profiles, is significant, and that the discharge is found to be relatively close to the P-B stability boundary. Therefore this analysis remains inconclusive.

Unfortunately, we did not obtain sufficiently well resolved pedestal profiles to allow for a linear peeling ballooning stability analysis using the ELITE code for all the measured pedestal profiles in the database. Instead we use the EPED model [28, 29] which predicts the pedestal height and width using calculated peelingballooning and kinetic ballooning mode (KBM) constraints. For this large dataset, we use the efficient EPED1 version of the model, which employs a simplified KBM constraint $\Psi = 0.076 \sqrt{\beta_{pol,ped}}$, where the pedestal width Ψ is defined to be the average of the ne and Te widths in normalized poloidal flux . EPED1 couples this KBM constraint with a full (width dependent) calculation of the peeling-ballooning mode stability using the ELITE code on sets of model equilibria to determine the pressure pedestal width and height self consistently.

The ratio of EPED1 predicted to observed pedestal pressure for the all baseline and hybrid CFC plasmas is 0.97 ± 0.21, with a correlation coefficient of 0.86 between predicted and observed pedestal height [3]. This standard deviation of 0.21 is in a typical range for studies of EPED model accuracy on several tokamaks [9, 29], which typically find agreement within ±20-30%). A comparison of EPED1 predictions to observed pedestal height for both ILW and CFC cases is shown in Figure 8. For 182 ILW low and 86 high triangularity baseline cases (Figure 8, left), the ratio of predicted to observed pedestal pressure is 1.06 ±0.22, with a correlation coefficient of 0.91. For 64 hybrid cases (Figure 8, right), the ratio of predicted to observed pedestal pressure is 1.02 ±0.15, with a correlation coefficient of 0.76. Note that for the ILW cases, the measured pedestal height is approximated as $2n_{e,ped}\ T_{e,ped}$, while for the CFC cases, the measured total pressure $P_{tot,ped}$ (electron + ion) at the pedestal top location is used. The good agreement and strong correlation with the EPED model predictions for the ILW cases (and CFC cases) suggest that these discharges are up against P-B and KBM constraints, as expected for the Type I ELM regime. While both CFC and ILW cases agree well with the model, the ratio of EPED-predicted to observed pedestal height is slightly higher for ILW than for CFC cases. This may be partially explained by reduced impurity dilution in the ILW cases, but other effects, such as modification of the bootstrap current with changing impurity characteristics may be important, and further study of these effects is planned.

CONCLUSIONS & DISCUSSION

The main reason for the confinement reduction in plasmas in the ILW is the reduction in pedestal pressure. This sets the boundary condition for the core and under stiff core profile conditions the

global confinement is affected. In the hybrid plasmas the loss of pedestal confinement is compensated by a steepening of the core profiles, and as a consequence the global confinement can approach that achieved in JET-C. In the absence of ion temperature measurements we assume $T_i = T_e$. This is justified by the relatively high plasma densities in JET-ILW, such that the ion-electron heat exchange time is low compared to the energy confinement time, but this assumption needs to be verified with actual T_i / T_e measurements when available.

The difference in wall composition leads to a change in impurity composition and radiation pattern. An increased Z_{eff} in the pedestal region leads to ion dilution and secondly affects edge current distribution. A peaked Z_{eff} profile at the separatrix is likely to change the stability results from that shown in Figure 7 (right) where a flat profile was used. In [8] experiments are reported with N_2 seeding. Replacing Carbon with Nitrogen as a divertor radiator and impurity indeed can affect the pedestal confinement indicating the importance of the role of the impurity composition.

Furthermore the core profile stiffness can be affected by the core rotation and/or rotation gradients [20]. Currently no rotation profiles are available and a detailed study of core profile stiffness will be conducted as soon as measurements are available. Finally the role of the impurity composition on core profile stiffness needs to be studied carefully. The results presented in this paper show the important role of JET ILW experiments to guide predictive modelling of ITER scenarios.

ACKNOWLEDGEMENTS

This work was partly funded by the RCUK Energy Programme under grant EP/I501045 and the European Communities under the contract of Association between EURATOM and CCFE and carried out within the framework of the European Fusion Development Agreement. The views and opinions expressed herein do not necessarily reflect those of the European Commission.

REFERENCES

[1]. Y. Andrew et al., Plasma Physics and Controlled Fusion, **48** (2006) 479.
[2]. MNA Beurskens et al, Nuclear Fusion **49** (2009) 125006
[3]. MNA Beurskens et al., submitted to Nuclear Fusion
[4]. L. Frassinetti et al., 37th EPS Conference on Plasma Physics, 2011 Dublin, Ireland, P1.1031.
[5]. L. Frassinetti et al., 39th EPS Conference on Plasma Physics, 2012 Stockholm, Sweden.
[6]. L. Frassinetti et al. Review of Scientific Instruments **83**, 013506 (2012)
[7]. C. Giroud et al, Nuclear Fusion **52** (2012) 063022
[8]. C. Giroud et al, This conference
[9]. R. Groebner, This conference
[10]. J. Hobirk et al, Plasma Physics and Controlled Fusion **54** (2012) 095001
[11]. L.D. Horton et al., 26th EPS Conference on Controlled Fusion and Plasma Physics (Maastricht) 1999.
[12]. International Conference of Plasma Surface Interaction, Aachen, 2012

[13]. Igitkhanov Yu and Pogutse O 2000 Contribution to Plasma Physics **40** 368
[14]. ITER Physics basis, Nuclear Fusion **39** No 12 (December 1999) 2175-2249
[15]. C.F. Maggi et al., 38th EPS Conference on Plasma Physics (Strasbourg) 2011.
[16]. E. Joffrin et al., Proceedings of the 23nd IAEA Fusion Energy Conference, Daejon, Republic of Korea (2010). Paper EX/1-1 http://www-pub.iaea.org/mtcd/meetings/PDFplus/2010/cn180/cn180_papers/exc_1-1.pdf
[17]. E. Joffrin et al, This conference
[18]. A Loarte et al, Plasma Physics and Controlled Fusion **45** (2003) 1549–1569
[19]. C.F. Maggi et al., 39th EPS Conference on Plasma Physics (Stockholm) 2012.
[20]. P. Mantica et al. Physical Review Letters 107, 135004 (2011)doi:10.1103/PhysRevLett.107.135004
[21]. Y. Martin et al., Journal of Physics: Conference Series **123** (2008) 012033.
[22]. International Conference of Plasma Surface Interaction, Aachen, 2012
[23]. Pasqualotto R. Et al., Review of Scientific Instruments **75**, 3891 (2004)
[24]. T. Pütterich et al., This conference
[25]. S. Saarelma et al, Plasma Physics and Controlled Fusion **51** (2009) 035001
[26]. Sartori R et al. 2004 Plasma Physics and Controlled Fusion **46** 723
[27]. P. Snyder et al, Nuclear Fusion **44** (2004) 320–328
[28]. P. Snyder et al, Physics of Plasmas **16**, 1 2009
[29]. P. Snyder et al, Nuclear Fusion **51** (2011) 103016

Wall	**Baseline low δ** $\delta_{av} \sim 0.28$	**Baseline high δ** $\delta_{av} \sim 0.36–0.45$	**Baseline low δ** $\delta_{av} \sim 0.2–0.25$	**Baseline high δ** $\delta_{av} \sim 0.35$
Carbon	I_p = 1.0–3.0MA q_{95} = 2.8–3.5	I_p = 1.0–2.5MA q_{95} = 3.3–3.6	I_p = 1.7–1.9MA q_{95} = 3.6–4.0	I_p = 1.4–1.9MA q_{95} = 3.6–4.5
Be/W	I_p = 1.2–3.5MA q_{95} = 2.8–4.1	I_p = 1.7–2.5MA q_{95} = 3.3–3.6	I_p = 1.7–2.0MA q_{95} = 3.6–4.0	I_p = 1.5–1.7MA q_{95} = 3.6–4.5

Table 1: Range of current and q_{95} for the ILW and C-wall H-mode database

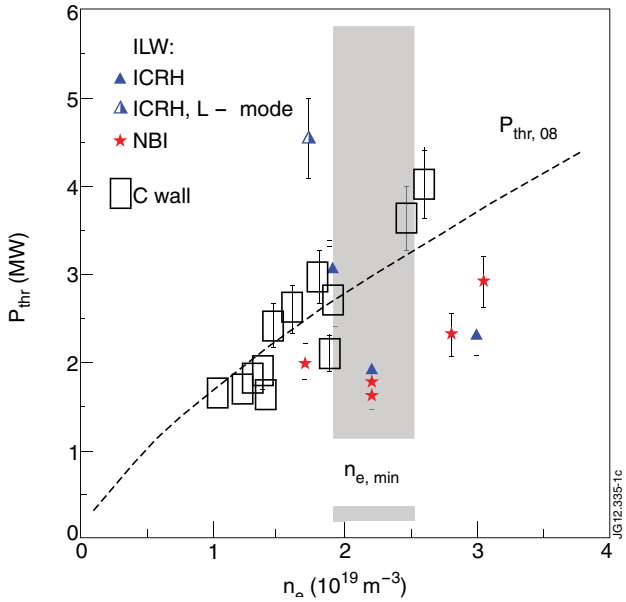

Figure 1: L-H power threshold P_{thr} at 1.8T/1.7MA for C and Be/W wall datasets. The threshold at low density is higher for the ICRH heated plasmas compared to the NBI heated plasmas as main plasma radiation is increased.

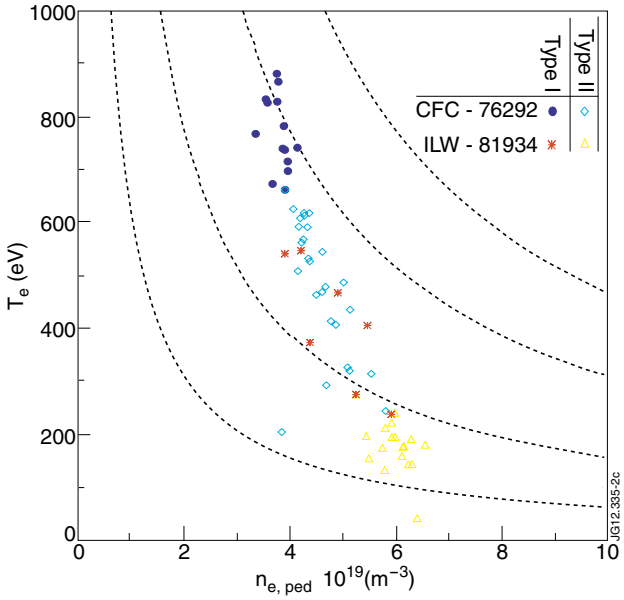

Figure 2: Pedestal temperature and density during a density ramp experiment with B_t = 3T an I_p = 2MA for C-wall and ILW. Full symbols are type I ELMs, open symbols are Type III ELMs.

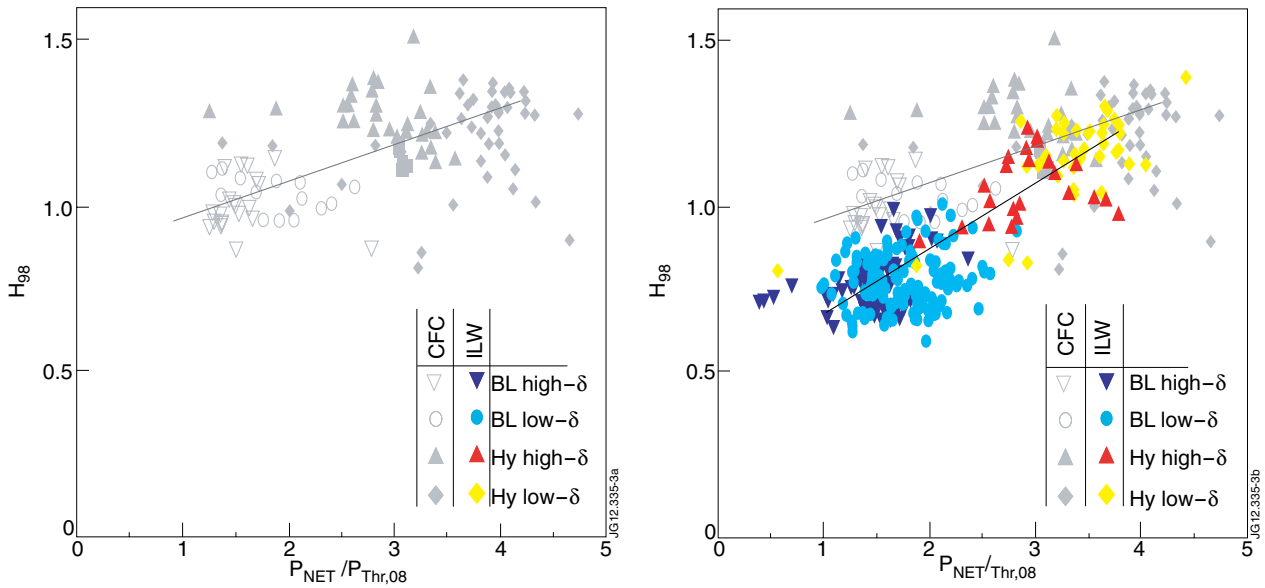

Figure 3: H_{98} versus the ratio of $P_{net}/P_{thr,08}$ for JET-C (left) and JET-ILW Hybrid and baseline ELMy H-mode plasmas overlaid (right). Note that the actual P_{thr} as measured in the dedicated ILW experiments is lower than $P_{thr,08}$. The two lines are linear fits to the data.

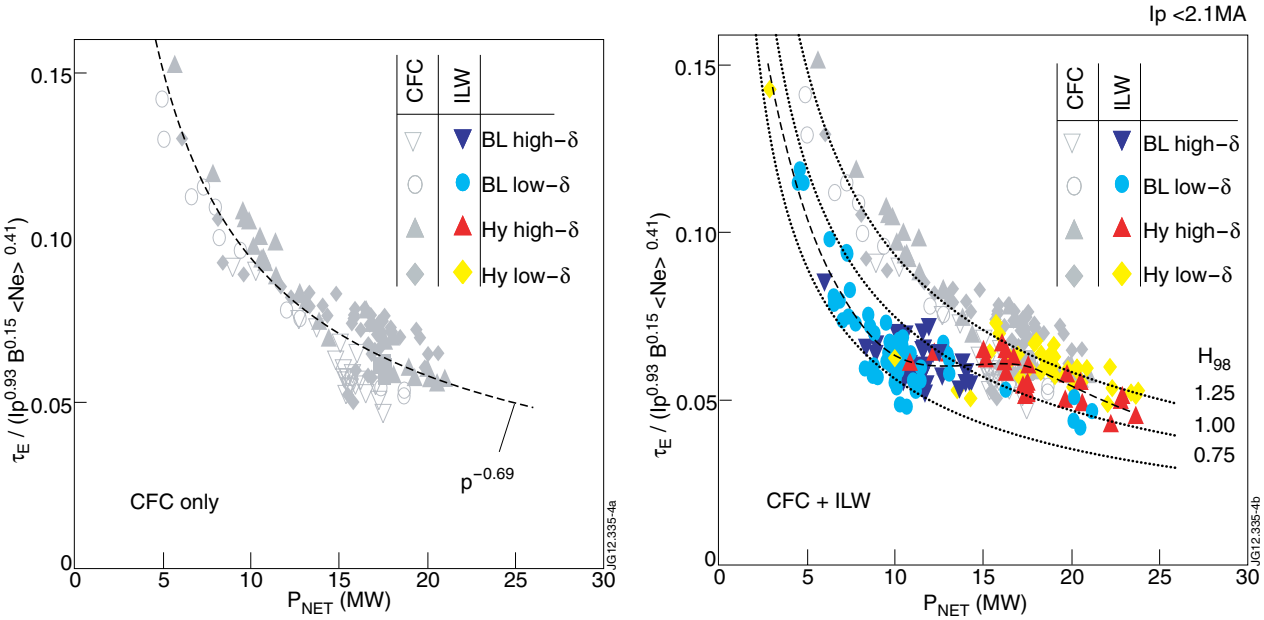

Figure 4: power degradation of the confinement for a) JET hybrid and baseline plasmas with the CFC wall (left) with the ILW data (I_p<2.1MA) overlaid (right).

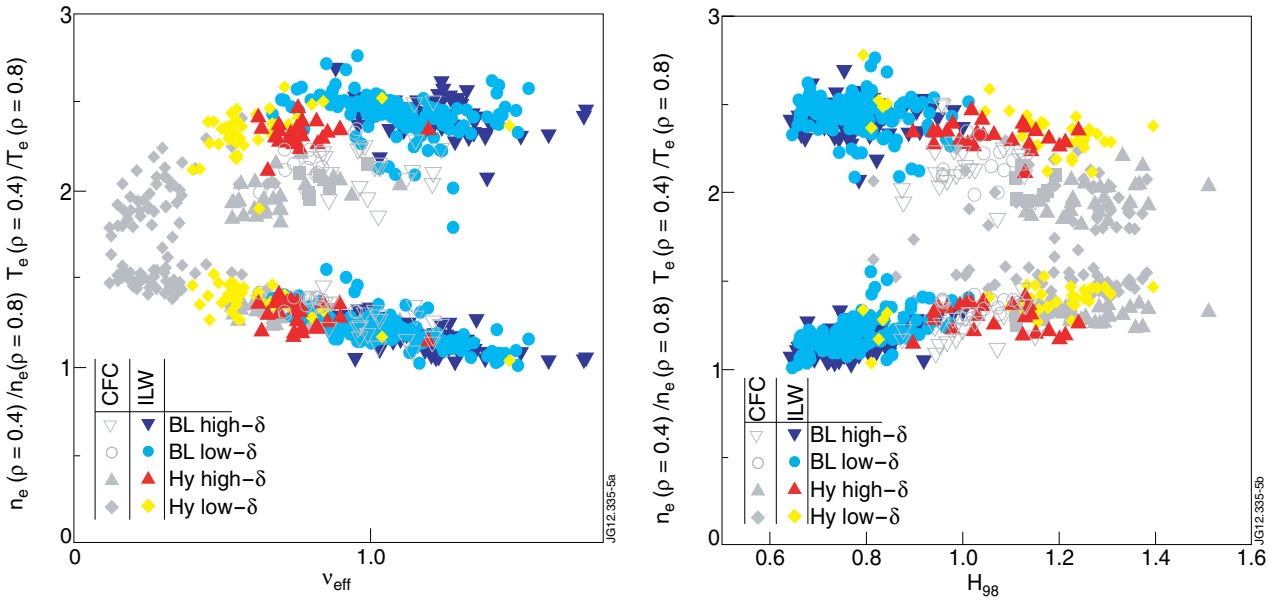

Figure 5: Profile peaking for the electron temperature and density versus collisionality (left) and confinement enhancement factor H_{98} (right)

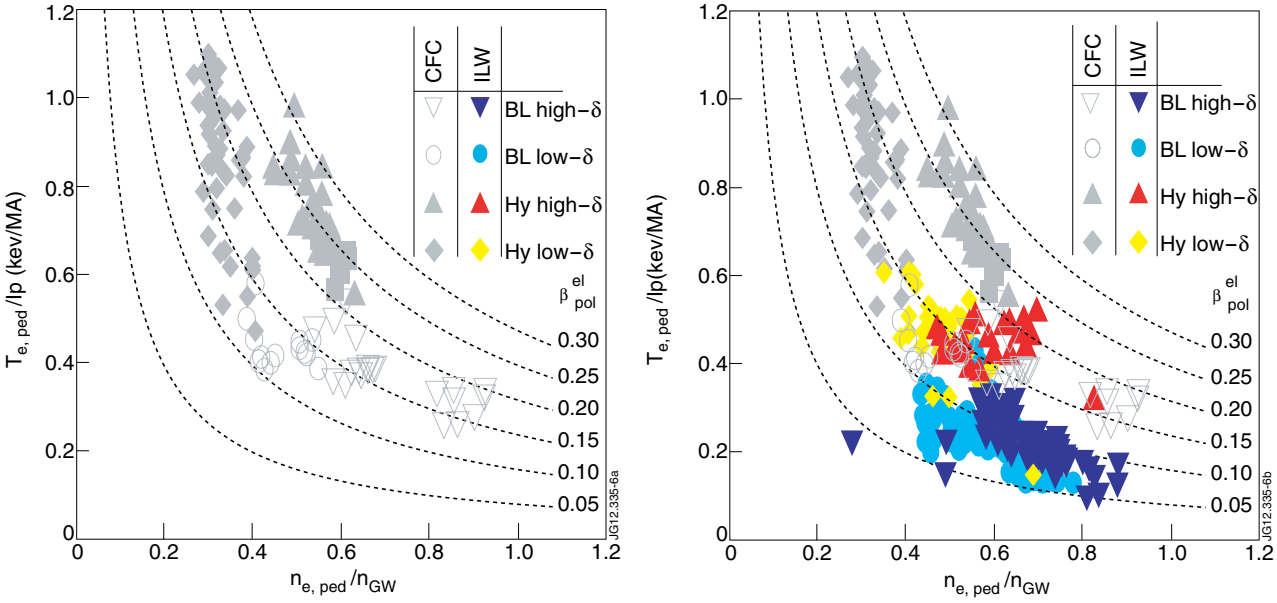

Figure 6: Pedestal T_e and n_e diagram normalised to I_p^2 as T_e/I_p and $n_{e,ped}/n_{gw}$ for JET-C Hybrid and baseline ELMy H-mode plasmas (left) and JET-ILW plasmas overlaid (right).

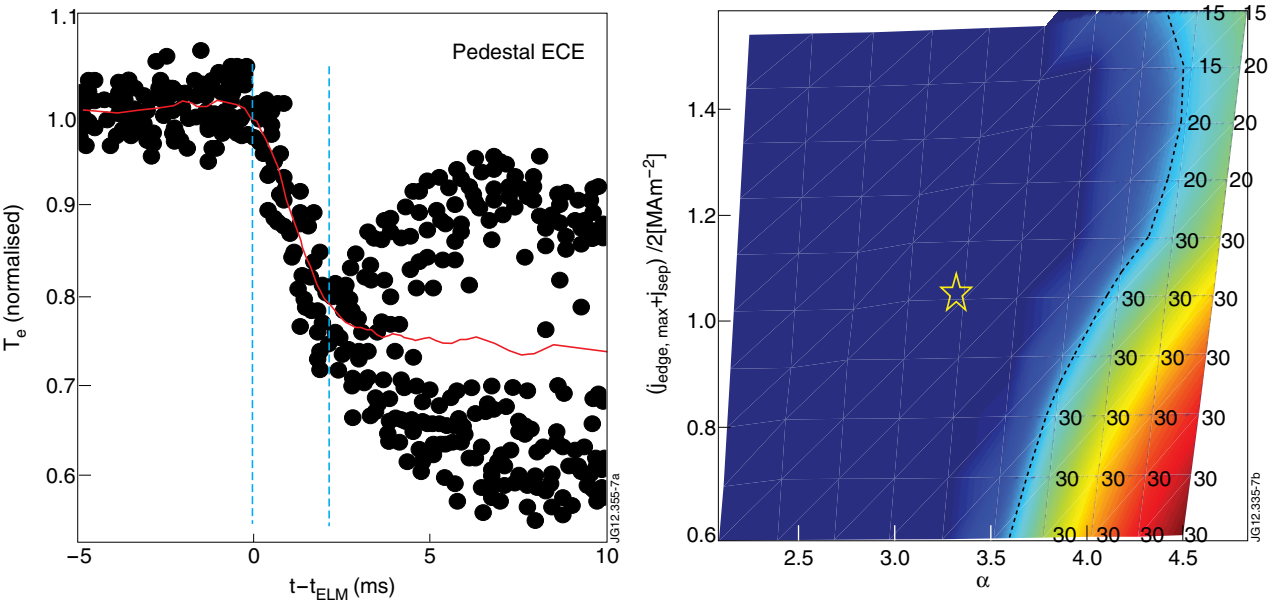

Figure 7: (left) ELM collapse time scale and (right) Peeling Ballooning stability for a typical ILW Type I ELMy H-mode with I_p/B_t = 2.5MA/2.7T high triangularity (δ~0.42, P_{net} = 15MW, Γ_D=3×10^{22} el/s) baseline plasma (Pulse No: 82806).

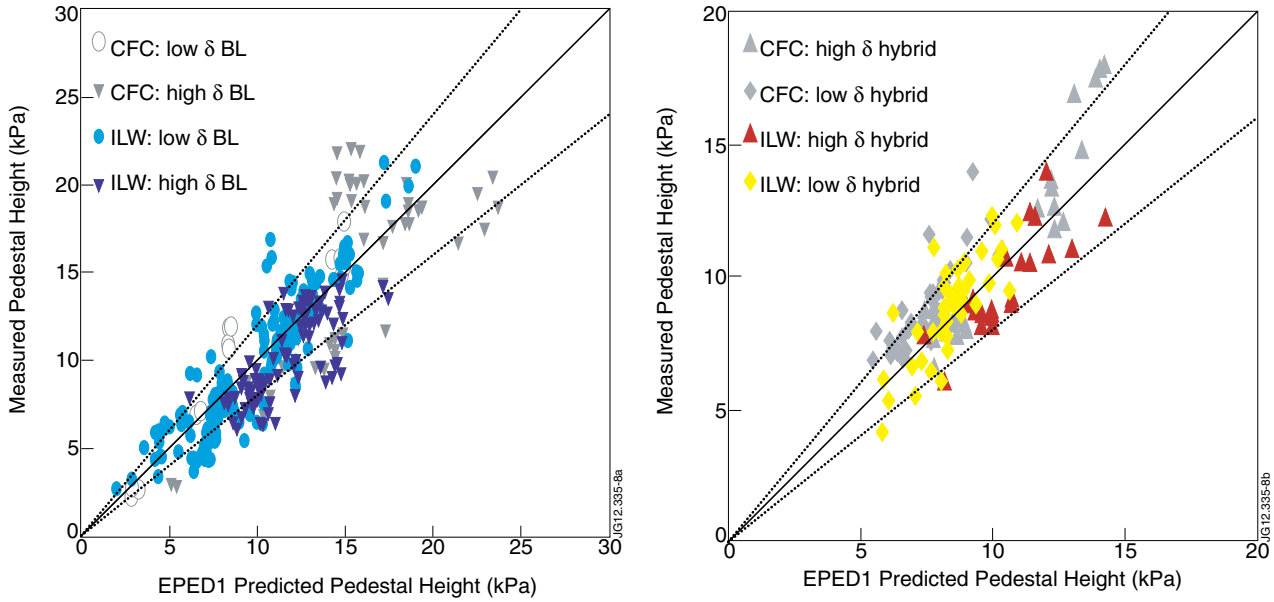

Figure 8: EPED1 predictions for the pedestal height compared to measured values for baseline plasmas (left) and hybrid plasmas (right) for CFC (grey) and ILW (coloured). The solid line indicates agreement, and the dashed lines ±20%.